# Micro- and Macro-phase Behavior in Protein-polyelectrolyte Complexes

Kevin W. Mattison, Yingfan Wang, Kris Grymonpré, and Paul L. Dubin*

Department of Chemistry, Indiana University - Purdue University, Indianapolis, IN 46202, USA

SUMMARY. Negatively charged polyelectrolytes such as carboxymethylcellulose, pectin, and alginate are commonly present in food products. These polyelectrolytes serve a variety of functions such as controlling viscosity and stabilizing emulsions. Proteins are also present in many food formulations. Because of their high charge density, polyelectrolytes can be expected to interact with these proteins. Hence, an understanding of the parameters controlling protein-polyelectrolyte interactions is useful.

The formation of protein-polyelectrolyte complexes (PPCs) is driven by electrostatic interactions, and electrostatic parameters such as protein surface charge density, polymer linear charge density, and ionic strength can influence both the formation and the stability of the PPC. However, the electrostatic attractive forces in PPCs are countered by a loss in polyelectrolyte conformational freedom. Hence, polymer chain parameters, e.g. the inherent chain stiffness (bare persistence length), are also important. For some protein-polyelectrolyte systems, the loss of polymer conformational freedom can become so large as to overcome electrostatic effects and prohibit PPC formation.

In addition to electrostatic effects, the structure of PPCs is also controlled by stoichiometry, i.e. the average number of bound proteins per polymer chain (n) increases with total protein concentration. At the same time, changes in the pH and ionic strength will be reflected in the mass action equilibrium constant, with an increase in the electrostatic interaction energy shifting the equilibrium ($Pr_{Unbound} \rightarrow Pr_{Bound}$) toward the bound state.

Macroscopic phase separation can arise when PPCs are intrinsically insoluble due to local charge neutralization. It can also be a consequence of the aggregation of electroneutral soluble PPCs. Hence, an understanding of the interactions and composition of the soluble complexes will enhance our ability to predict and control phase behavior in protein-polyelectrolyte systems.

 CCC 1022-1360/99/$ 17.50+.50/0

## Introduction

"Gums" or "hydrocolloids" are used in many food products to bind water, control viscosity, stabilize emulsions, and influence an array of rheological and surface properties. Many of these compounds, for example carboxymethylcellulose, pectin, alginates, xanthans, and carrageenan, are negatively charged polyelectrolytes. Consequently, they may be expected to bind strongly any cationic species present, especially ones of high net charge. Since proteins are present in many of these systems, the properties and behavior of such polyelectrolytes in food systems can be expected to be influenced more by their interactions with charged (amphoteric) proteins than by their interactions with uncharged molecules such as oils, sugars and starches, or molecules of like charge, such as lipids. A specific example is the association of carageenan with casein in dairy products. Because polyelectrolyte-protein complexes may exist in several states, such as soluble complexes, amorphous precipitates, coacervates, or even gels, the phase effects of polymeric food additives could in large part depend on the properties of their complexes with proteins. Studies of proteins and polyelectrolytes in simple buffer or salt solutions yield fundamental information impossible to obtain by measurements with complicated food formulations. This report focuses on the solubility behavior of mixtures of strong polyelectrolytes and proteins in simple model systems.

Protein-polyelectrolyte interactions are fundamental to numerous biological processes. A classic example is the synthesis of proteins in cellular systems, where every major step in the synthesis route is mediated by electrostatic and hydrophobic interactions between the macromolecular constituents. For example, Record *et al.*[1] and others have clearly shown how protein-DNA association is an integral step in DNA replication and gene regulation. Other biological polyelectrolytes also interact with proteins; Colby for example, has attempted to relate the formation of soluble complexes between bovine serum albumin (BSA) and hyaluronic acid in the synovial fluid to arthritic swelling and inflammatory joint disorders.[2]

The literature on complex formation between synthetic polyelectrolytes and proteins is more diffuse, since it lacks the focus provided by the context of molecular biology.[3] However, numerous studies on such complex formation and related phase separation effects have been motivated by potential industrial applications, such as protein separations,[4] enzyme stabilization and immobilization,[5] biosensor production,[6] and blood substitutes.[7] It is furthermore likely that an understanding of protein-polyelectrolyte phase phenomena will be central to the development of microencapsulated drug delivery devices[8] and to the use of polymeric scaffolds for tissue regeneration.[9]

The majority of the studies referenced above have focused on the characterization or utilization of a specific protein-polyelectrolyte system within a relatively small range of conditions, e.g. pH, ionic strength, and concentration. Thus, while these studies are invaluable in understanding specific protein-polyelectrolyte complexes and related phase phenomena, very few of them provide a systematic examination of the key physical parameters controlling the electrostatics of protein-polyelectrolyte complexation. Hence, it is difficult to form general conclusions that can be applied to all PPC systems. Such general understanding can form the basis for studies closer to food technology, by providing a conceptual framework that can be applied to a variety of polyelectrolytes used at different pH's, ionic strengths, and compositions, in the presence of different proteins.

Research in this laboratory has provided some clarification of the mechanisms responsible for phase separation in protein-polyelectrolyte systems. We have been able to show that (1) complex formation is driven by electrostatic interactions, with hydrogen bonding and hydrophobic effects being of secondary importance;[10] (2) soluble or primary complexes, composed of a single polymer chain with multiple bound proteins, are precursors to phase separation;[11] (3) bulk phase separation arises from the aggregation of electroneutral (insoluble) primary complexes;[11] and (4) other than a decrease in solubility, there are no discontinuities in the microscopic properties of the PPC during phase transitions.[12] Such observations justify a focus on fundamental studies of the soluble PPC, thereby avoiding the scattering and particle stability problems associated with multiphase systems. Since soluble

complexes are precursors to phase separation, an understanding of binding and composition within the soluble PPC should enhance our ability to predict and control phase behavior.

The main parameters controlling binding within the soluble PPC are ionic strength, protein surface charge density, and polymer linear charge density and flexibility. But the composition of the PPC is also subject to mass action and thus controlled by the bulk protein to polymer mass ratio, even though the mass action equilibrium constant is modulated by the aforementioned electrostatic parameters. Hydrophobic effects are typically reflected in the solubility of the primary complex and may lead to the formation of soluble aggregates. However, for most strong polyelectrolytes, hydrophobic effects are relatively small and their influence on phase separation is usually subtle.

In this report we present past and recent results from our laboratory, with a focus on the mechanisms of phase separation, and the influence of ionic strength, pH, mass action, and polyelectrolyte chain parameters on the binding and composition within the protein-polyelectrolyte complex. In order to simplify the model systems, we chose to work with the strong synthetic polyelectrolytes listed in Table 1.

**Table 1: Model Polyelectrolytes**

| Polyelectrolyte | Charge |
|---|---|
| Poly(dimethyldiallylammonium chloride) (PDMDAAC) | + |
| Poly(methacrylamidopropyltrimethylammonium chloride) (PMAPTAC) | + |
| Poly(acrylamidomethylpropylsulfonate) (PAMPS) | - |
| P(AMPS-acrylamide) copolymers ($PAMPS_{80}AAm_{20}$) | - |

The criteria for polyelectrolyte selection was 1) constant charge density, 2) availability of characterization data, e.g. molecular weight, polydispersity, linear charge density, and persistence length, and 3) commercial or synthetic availability. While the selection of these polyelectrolytes simplifies an examination of the electrostatic interactions in PPC systems in that the protein charge can be varied independently of polymer charge, it is fully recognized that more subtle pH effects may occur when using food-polyelectrolytes such as carboxylated polysaccharides. On the other hand, an examination of the interactions in these simple systems

should lead to a better understanding of more complex systems, and allow us to develop general principles and methodologies applicable to future work with polyelectrolytes in food chemistry. References to publications containing the experimental details and the instrumental techniques are given.

## Results and Discussion

The structures of the polyelectrolytes referenced throughout this report are shown in Figure 1. Appropriate references for the characterization data, e.g. weight and number average molecular weights, polydispersity, linear charge density, and persistence length, are cited in the Reference section. The latter two are also included in Table 2 of this report.

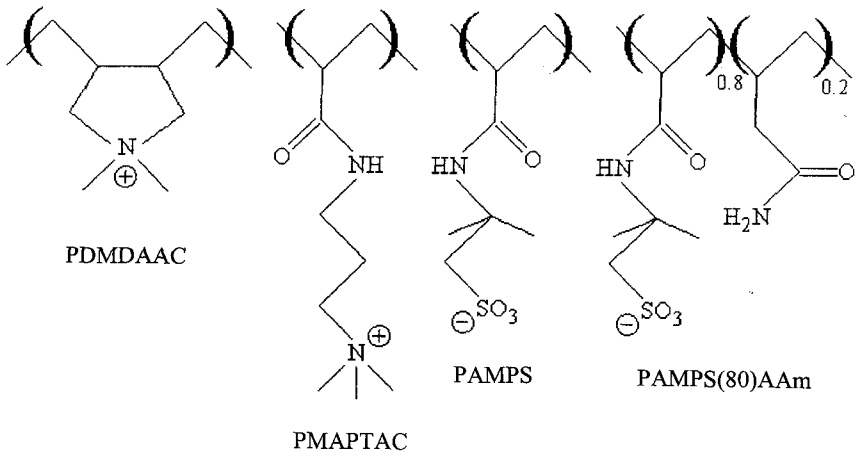


**Figure 1:** Structures for polycations, PDMDAAC and PMAPTAC, and polyanions, PAMPS and PAMPS(80)AAm.

*Phase Transitions: Effects of pH and Stoichiometry*

Figure 2 shows a typical pH-turbidimetric titration for BSA and PDMDAAC in 0.1 M NaCl. Since the polyelectrolyte is a polycation, the electrostatic interactions increase with pH. This figure can be presented in terms of three regions.[13] In region I ($pH < pH_c$), Coulombic repulsive forces between the positively charged protein and the positively charged polyelectrolyte prohibit the formation of complexes, and the turbidity is constant with pH. In

region 2, the primary or soluble complex region, the small increase in turbidity is representative of an increase in the concentration and/or the molecular weight of the scattering species. In region 3 (pH > $pH_\phi$), the sharp increase in turbidity indicates macroscopic phase separation. $pH_c$ and $pH_\phi$ then can be defined as critical pH values separating the three phases.

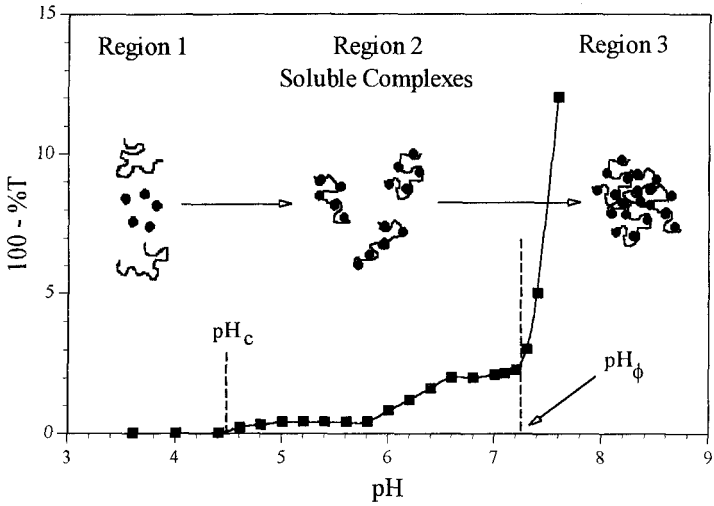


**Figure 2:** pH-turbidimetric titration of BSA-PDMDAAC in 0.1 M NaCl. [BSA] = 0.6 g/L and [PDMDAAC] = 0.12 g/L. $pH_c$ and $pH_\phi$ are critical pH values separating three distinct phases.

Since the increase in turbidity at $pH_c$ in Figure 2, on the order of 0.4 %T, is only four times larger than the instrumental error, it is reasonable to question the significance of this subtle effect. Figure 3 shows dynamic and static light scattering (A), turbidimetric (A), and potentiometric titration (B) results for BSA with another polycation, PMAPTAC, in 0.1 M NaCl.[10] The dynamic light scattering result is shown as the observed apparent Stokes radius, calculated from the mutual diffusion coefficient by assuming that interparticle interactions are negligible and applying Stokes law. The static light scattering result is reported as relative intensity at 90° scattering angle. Phenomenologically at least, $pH_c$ can be identified with some reliability. The absence of any effect of pH, for pH < $pH_c$, on 100 - %T, $R_S$, $I_{90}$, or $\Delta Z_{BSA}$ suggests that $pH_c$ may be viewed as a microscopic phase transition.

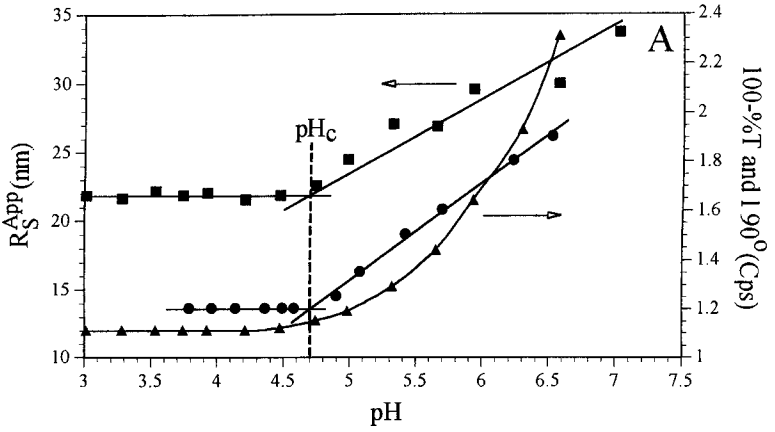


**Figure 3a:** $R_S^{App}$ (■), 90° scattering intensity (▲), and turbidimetry (●) results for BSA with PMAPTAC in 0.1 M NaCl. [BSA] = 0.6 g/L and [PMAPTAC] = 0.12 g/L. See text for explanation of $R_S^{app}$.

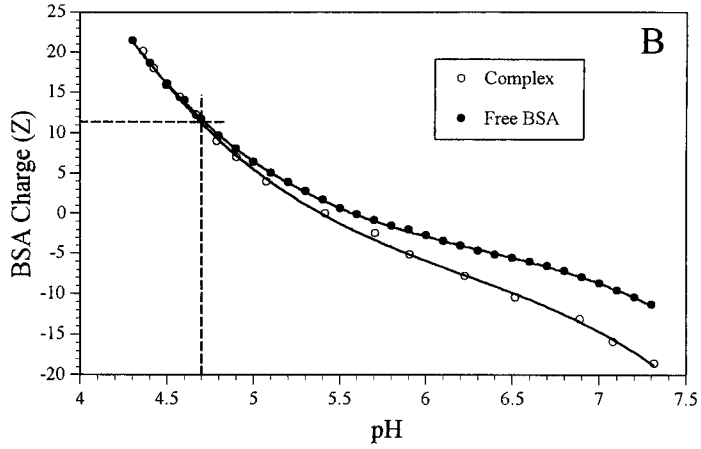


**Figure 3b:** Potentiometric titration results for BSA with PMAPTAC in 0.1 M NaCl. [BSA] = 0.6 g/L and [PMAPTAC] = 0.12 g/L.

*Stoichiometry and Mass Action*

The initiation of complex formation at $pH_c$ is independent of protein and polymer concentration.[13] The initiation of true phase separation, $pH_\phi$, is also independent of total

macromolecular concentration, but dependent upon the protein / polymer weight ratio (r). Figure 4 shows the effect of r on $pH_\phi$ for BSA-PDMDAAC in 0.1 M NaCl.[13]

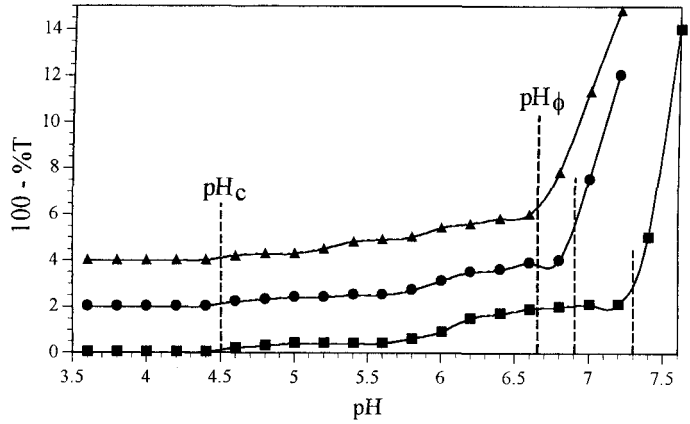


**Figure 4:** Influence of $r = (C_{pr}/C_P)$ 5 (■), 20 (●), and 100 (▲) on $pH_c$ and $pH_\phi$. Curves are offset for clarity.

The dependence of $pH_\phi$ on r can be explained if phase separation is a consequence of neutralization of the net charge of the primary complex ($Z_T$) which is given by Equation 1, where $Z_P$ is the total polymer charge (independent of pH and proportional to MW), n is the number of bound proteins per polymer chain, and $Z_{pr}$ is the pH dependent protein charge.[14]

$$Z_T = Z_P + nZ_{pr} \qquad (Z_T)_\phi = 0 \tag{1}$$

If protein binding at $pH > pH_c$ follows a mass action equilibrium, then n will increase with r. Consequently, the charge per protein molecule (negative) required to achieve complex neutralization decreases in magnitude, corresponding to a decrease in $pH_\phi$ with r. In their work with protein-polyelectrolyte systems, Okasaki *et al.* also attributed the r dependence of $pH_\phi$ to mass action effects.[15]

In contrast to our observation that $pH_\phi$ is independent of macromolecular concentration, Bungenberg de Jong[16] and Burgess[17] both observed a decrease in protein-polyelectrolyte coacervation at high concentration, implying that $pH_\phi$ depends on concentration. Burgess

attributed this decrease in PPC coacervation to entropic effects, in that as the solution concentration approaches that of the coacervate, the energy gained via coacervate formation is greatly reduced.[17] At the lower concentrations employed in our studies, these entropic effects should be negligible. Hence, comparison of the results may be problematic.

The electrophoretic mobility and turbidity for BSA-PDMDAAC at r = 10 in 0.02 M NaCl are shown in Figure 5, where pH has been converted to protein charge. While complex formation is initiated at $pH_c < pI$, bulk phase separation occurs only when the protein and polyelectrolyte are oppositely charged.[11] This observation is consistent with those of Burgess *et al.*, who also reported that PPC coacervation is prohibited for protein-polyelectrolytes with the same charge sign.[17,18] As evident in Figure 4, the PPC mobility becomes zero at the pH of maximum turbidity, consistent with the role of complex charge neutrality in coacervation.

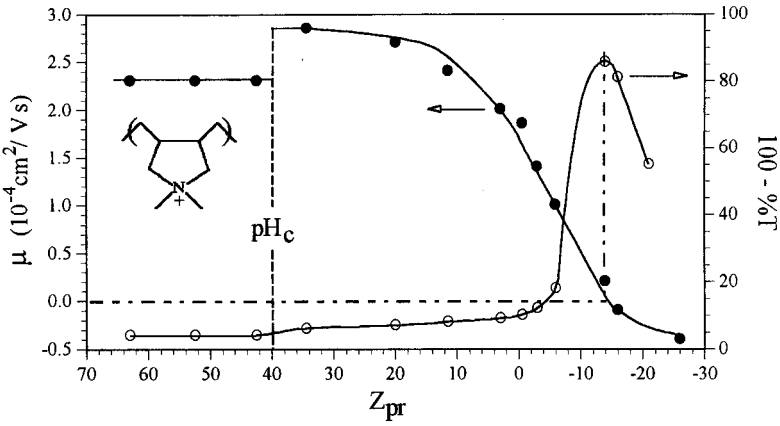


**Figure 5:** Electrophoretic mobility (●) and turbidimetry (O) results for BSA-PDMDAAC at r = 10 in 0.02 M NaCl. [BSA] = 3 g/L.

A turbidity maximum with respect to pH is characteristic of PPCs. A similar turbidity maximum is observed when r is varied at constant pH.[19] These maxima are consistent with Bungenberg de Jong[16] and Burgess[17,18], who reported r- and pH-dependent maxima in the coacervate yield. Burgess attributed these maxima to stoichiometric charge equivalence, based upon the observations that the maximum corresponded to a 1:1 charge ratio between

the components and that the PPC mobility went to zero at the point of maximum coacervate yield. Tsuboi *et al.* also reported a turbidity maximum, for protein-polyelectrolyte mixtures in the absence of salt, corresponding to the point of stoichiometric charge equivalence.[20]

The stoichiometry in a PPC coacervate may be determined by centrifugation to remove the coacervate, followed by measurement of the amount of free protein and polymer in the supernatant.[21] Results for BSA-PDMDAAC are shown as %BSA yield (BSA in the coacervate relative to the total BSA) as a function of r at various pH values in Figure 6.

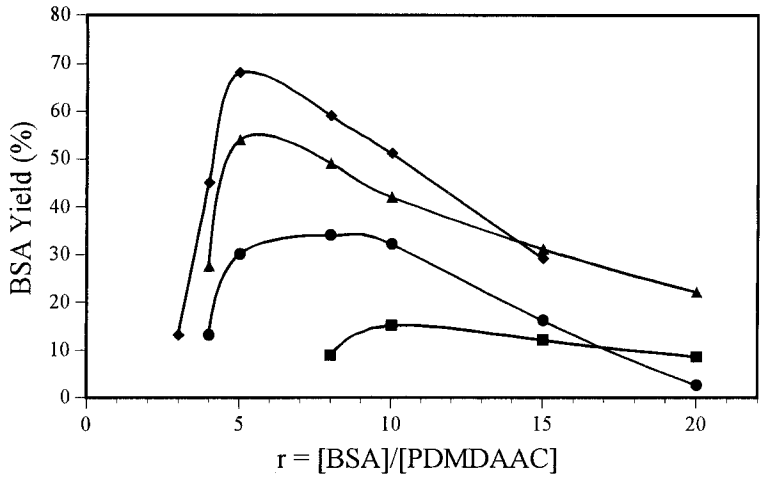


**Figure 6:** %BSA yield for BSA-PDMDAAC coacervate prepared in 0.1 M NaCl at pH 8.0 (■), 8.5 (●), 9.0 (▲), and 9.5 (◆).

The decrease in BSA yield for $r \neq r_{max}$ can be attributed to mass action effects and the solubility of the complex as follows. As r decreases relative to $r_{max}$, n also decreases, and the average charge on the primary complex becomes positive. This non-zero charge increases the solubility of the complex and subsequently decreases the amount of coacervate removed from the system. The net result is a decrease in both the amount of coacervate and the number density of BSA within the coacervate. When r increases relative to $r_{max}$, n increases, the average charge becomes negative, and the complex again becomes more soluble. In this case

however, the protein density within the coacervate increases, which offsets the decrease in BSA yield arising from the loss of coacervate. Hence the lack of symmetry in Figure 6.

The %BSA yield in Figure 6 tends to increase with pH, from which we might infer that n also increases with pH. Calculation of n (at $r_{max}$), from the protein concentration in the supernatant, indicates a threefold increase (7 to 20) as the pH is increased from 8.0 to 9.5. The calculations are simplified by Wang *et al.*'s observation that the polymer concentration at $r_{max}$ is negligible.[21] In contrast to the stoichiometric charge equivalence implicit in Equation 1 and reported by both Burgess and Tsuboi, an n value of 20 at pH 9.5 corresponds to a net protein charge (negative) equivalent to only 50% of the polyelectrolyte charges. At pH 8.0 this value is reduced to 15%. The conflicting results may be a consequence of ion adsorption. At the low and zero ionic strengths employed by Burgess and Tsuboi respectively, ion adsorption would be either negligible or absent. At moderate ionic strength, counterion condensation and ion adsorption could be significant. In its present form then, Equation 1 is strictly correct only for PPC systems in the absence of salt. When salt is present, adsorbed ions will contribute to the net charge on the PPC ($Z_T = Z_P + nZ_{pr} + f_A Z_{ion}^- + f_C Z_{ion}^+$).

Since soluble complexes are precursors to coacervate, the microscopic stoichiometry of the former might be retained upon formation of latter. The composition and structure of the soluble complex can be studied by a number of scattering techniques, including dynamic light scattering (DLS). Figure 7 shows the distribution of diffusion coefficients from DLS for BSA-PDMDAAC at r = 10 in pH 8.1, 0.16 M NaCl.[11] The inset in Figure 7 shows the Stokes radius of the PPC as a function of r. The bimodal distribution, with corresponding $R_S^{app}$ values of 29 and 3.5 nm, is typical for protein-polyelectrolyte systems at high r. Due to the intense scattering of the complex, polyelectrolytes are effectively invisible in DLS studies of protein-polyelectrolyte mixtures. Therefore, the larger peak in this figure ($R_S^{app}$ = 29 nm) is representative of the soluble PPC. At low r, the protein peak (3.5 nm for BSA) disappears, indicative of mass action effects and a strong binding constant. In protein-free solutions at this ionic strength, PDMDAAC has a measurable $R_S^{app}$ value of 25 nm. The similarity of the $R_S^{app}$ values for the soluble PPC and the polyelectrolyte is supportive of Xia[22] and Zaitsevs'[23] proposals that the primary complex is composed of a single polymer chain with multiple bound

proteins. The results are also consistent with the observations of Tan *et al.*, who reported that the soluble protein-polyelectrolyte complex had a hydrodynamic radius approximately 15% larger than that of the free polyelectrolyte.[24]

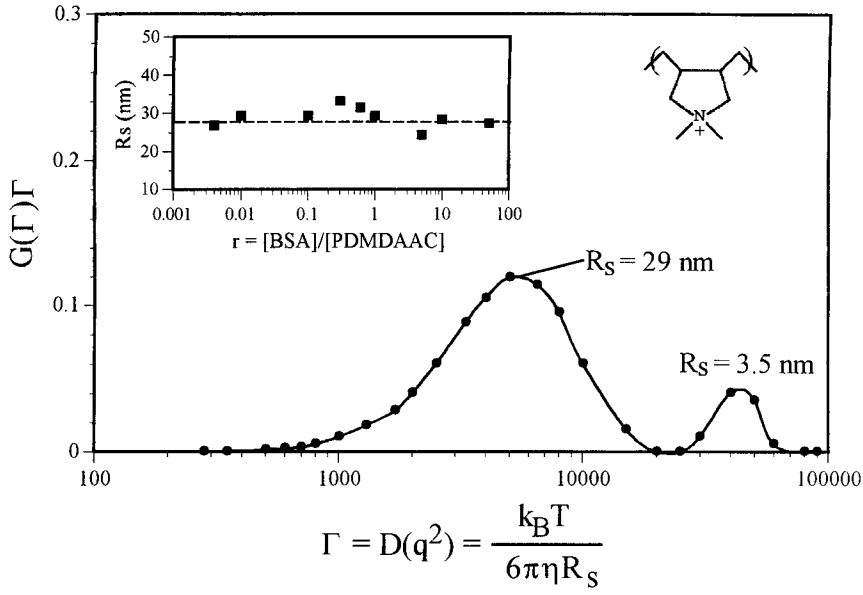


**Figure 7:** Dynamic light scattering (DLS) data showing bimodal distribution of diffusion coefficients. Inset shows effect of r = [Protein]/[Polymer] on the hydrodynamic radius of soluble BSA-PDMDAAC in pH 8.1, 0.16 M NaCl.

The independence of $R_S^{app}$ (Figure 7 inset) with r implies that the conformational structure of the polyelectrolyte within the PPC is controlled by the polymer chain parameters, and is independent of the number of proteins bound to the polymer. This observation is consistent with that of Gao *et al.*, who found that the polyelectrolyte conformational structure was independent of both the number and the type of protein bound.[25]

In contrast to DLS, the electrophoretic light scattering (ELS) of PPCs contains signals from both the complex and the free polymer, while the protein is effectively invisible.[11] Figure 8

shows the mobility (μ) *vs.* r results for BSA-PDMDAAC under the same conditions as those employed in Figure 7. The inset in Figure 8 shows the corresponding scattering intensity.

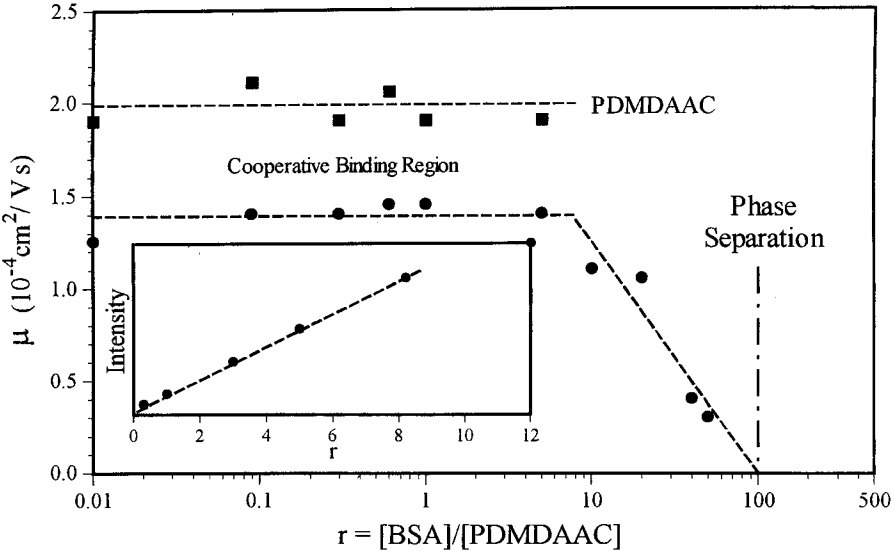


**Figure 8:** Effect of r on the electrophoretic mobility (μ) and the 90° scattering intensity of BSA-PDMDAAC in pH 8, 0.16 M NaCl. PPC (●), PDADMAC (■).

Since the scattering intensity is proportional to both the weight concentration and the molecular weight of the complexes, $C_X$ and $M_X$ respectively, the linearity of the intensity in Figure 8 suggests that $M_X$ is constant for $r \leq 8$, while $C_X \propto r$ as long as free polymer is present (low r). The constant mobility for $r \leq 8$ indicates that the charge density of the PPC is also constant. Additionally, the loss of the polymer ELS signal at $r > 10$ implies that the concentration of PDMDAAC at $r > 8$ is effectively zero. The results of Figures 7 and 8 can be understood if BSA binds cooperatively to PDMDAAC at low r, resulting in a mixture of soluble complex and free polyelectrolyte. At higher r values, the cooperativity is lost and the main solution components are soluble complex and free protein.

Cooperative binding of BSA to polyelectrolytes was also observed by Kabanov *et al.* using ultracentrifugation.[26] From size exclusion chromatography, Xia *et al.* reported cooperative

binding of lysozyme to PDMDAAC.[27] Gao *et al.* calculated the binding density of BSA and β-lactoglobulin with sodium poly(styrene sulfonate) (NaPSS) by capillary electrophoresis, and reported that β-lactoglobulin binds in a cooperative fashion.[25] In the same study however, Gao observed non-cooperative binding for BSA with NaPSS.

The effects of pH on PPC phase behavior arise from the dependence of protein charge on pH. The expected correlation between the magnitude of protein binding and pH is evident in Figure 9, which shows the 90° scattering intensity results for the soluble BSA-PDMDAAC complex in 0.1 M NaCl at r = 1. The total concentration of PDMDAAC was varied by diluting the solutions with 10% phosphate buffer at the reported pH. Hence, no change in r.

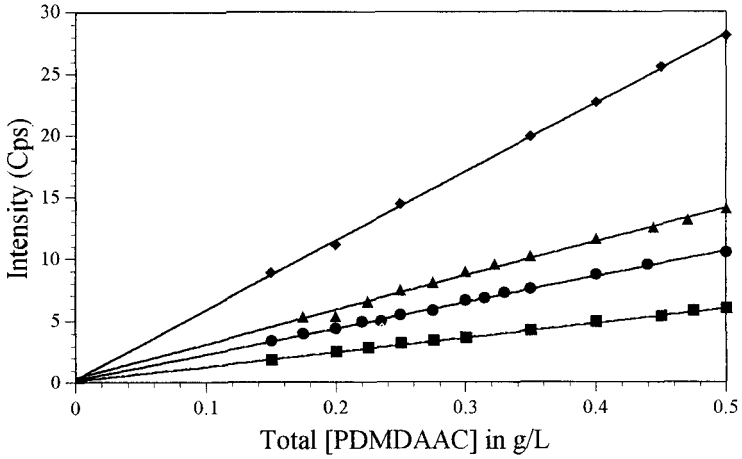


**Figure 9:** SLS results for BSA-PDMDAAC at r = 1 in 0.1 M NaCl at pH 6.4 (■), 7.1 (●), 7.5 (▲), and 8.5 (◆).

The linearity of the data in Figure 9 indicates that $M_X$ is independent of polymer concentration at constant pH and r. Additionally, the pH dependent slope is consistent with a pH dependent molecular weight, indicating that $M_X$ increases with pH for protein-polycation systems and vice versa for protein-polyanion systems.

From the neutrality expression (Eq. 1), we would expect the net protein charge to control the pH of bulk phase separation ($pH_\phi$). However, the total charge on the soluble PPC is also dependent upon n, the number of proteins bound to the polymer chain. It is difficult therefore to deconvolute the influence of mass action from that of the net protein charge at bulk phase separation. We can however state that the pH modulates the intrinsic protein binding constant and subsequently the number of proteins bound to a single polymer chain; which, in conjunction with the pH dependent net protein charge controls the solubility of the primary protein-polyelectrolyte complex.

*Ionic Strength Effects*

Electrostatic shielding effects should cause $pH_c$ and $pH_\phi$ for protein-polycationic systems to increase with increasing ionic strength, as is indeed seen in Figure 10 for BSA-PDMDAAC.[13]

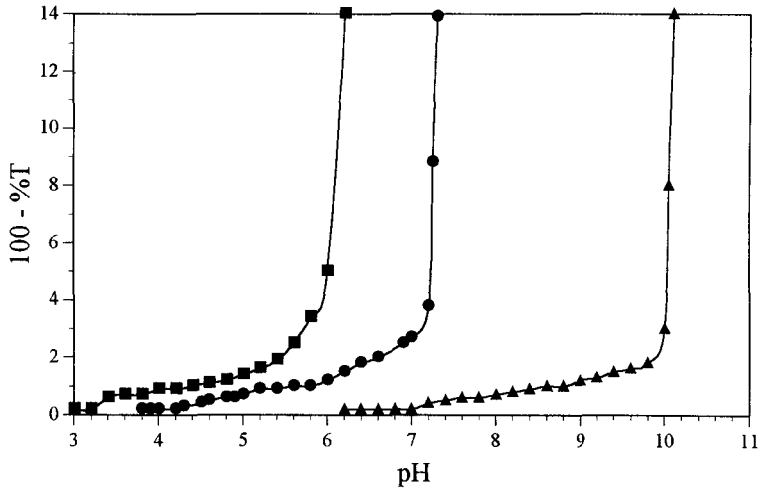


**Figure 10:** Influence of ionic strength on $pH_c$ and $pH_\phi$ for BSA-PDMDAAC with [BSA] = 0.6 g/L and r = 5. I = 0.02 (■), 0.08 (●), and 0.2 (▲).

The dependence of $pH_c$ and $pH_\phi$ on I may be represented by two phase boundaries which, as shown in Figure 11, separate the non-associative, primary complex, and coacervate regions.[13] The lower curve in this figure is the $pH_c$ boundary, which is independent of r,[13] and the upper curve is the $pH_\phi$ boundary for r = 5.

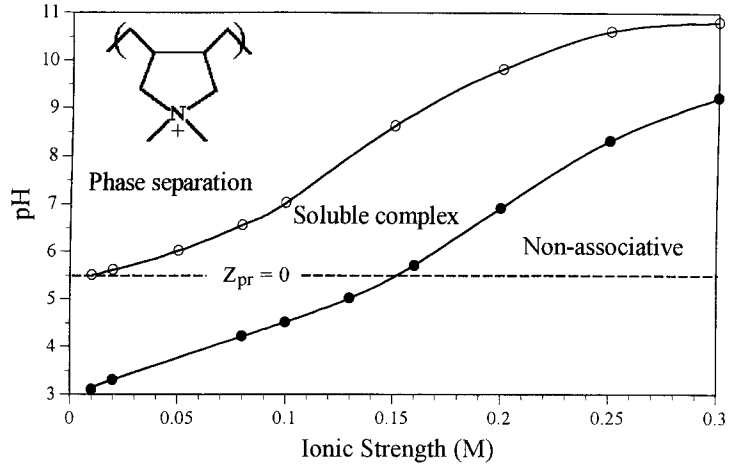


**Figure 11:** Phase boundaries for BSA-PDMDAAC at [BSA] = 0.6 g/L and r = 5. pHc (●), pHf (O).

Figure 12 shows the BSA-PDMDAAC phase boundary data plotted as $Z_{pr}$ (net BSA charge) versus $I^{½}$. The $(Z_{pr})_{\phi}$ phase boundary for BSA-PMAPTAC is included for comparison.

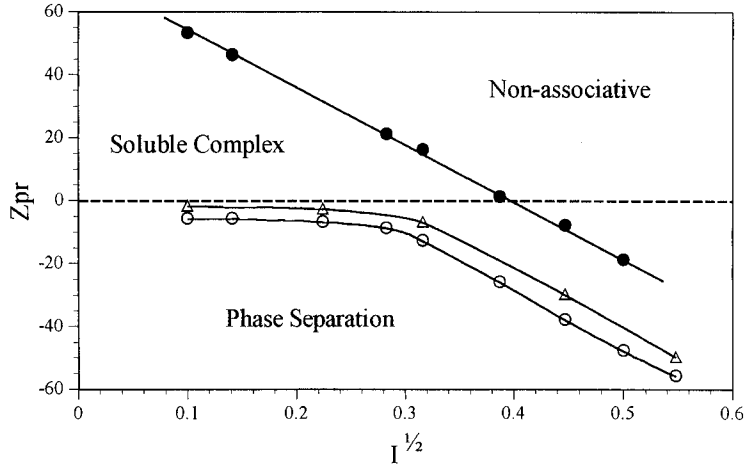


**Figure 12:** Phase boundary data plotted as $Z_{pr}$ *vs.* $I^{½}$ for BSA with PDMDAAC, $Z_c$ (●) and $Z_{\phi}$ (O), and PMAPTAC, $Z_{\phi}$ (Δ).

The linearity of $(Z_{pr})_c$ with $I^{½}$ is consistent with non-specific electrostatic shielding by NaCl. This observation is also consistent with theoretical models for polyelectrolyte adsorption developed by Muthukumar,[28,29] Manning,[30] and Fleer,[31] all of which predict a critical surface charge density proportional to the Debye-Hückel parameter ($\kappa$). The continuity of the $(Z_{pr})_c$ data through $Z_{pr} = 0$ and the observation that binding readily occurs on the wrong side of pI indicate that there is no special significance of pI, and that protein-polyelectrolyte complex formation is initiated at charged patches on the protein surface. Similar results were obtained by Tan *et al.*, who reported the binding of two polyanions, poly(acrylamidomethylpropyl sulfonate) (PAMPS) and NaPSS with negatively charge gelatin at high pH.[24]

The data in Figure 12 also imply that the surface charge density of the patch is proportional to the global protein charge, even though binding is initiated when the protein and polyelectrolyte have the same charge sign. This result is examined in detail in reference 10. Suffice it here to state that the binding patch may be small, but that the number of patches should increase with the size of the protein. For larger proteins, the average charge density of the patch might then be proportional to the global protein charge.

The asymptotic approach of the $(Z_{pr})_\phi$ boundaries to $Z_{pr} = 0$ at low I in Figure 12 is supportive of the neutrality assumption ($Z_T = 0$ at $pH_\phi$), in that phase separation is prohibited when the protein charge has the same sign as the polyelectrolyte. However, since the linear charge density of PMAPTAC is twice that of PDMDAAC, the observation that BSA-PMAPTAC exhibits phase separation at lower protein charge (less negative) appears to contradict Equation 1; unless of course the increase in linear charge density leads to an increase in the binding constant and a subsequent increase in the number of proteins bound per polymer chain. It could be argued that this increase in n is a result of differences in polymer chain stiffness, but the similarity of the two $(Z_{pr})_\phi$ boundaries at all ionic strengths would tend to discount this argument, in that polyelectrolyte persistence lengths are strongly dependent upon both the ionic strength and the linear charge density.[32] The hypothesis that n increases with polymer linear charge density is consistent with Okasaki *et al.*, who reported that the number of proteins bound and hence $pH_\phi$, was dependent upon the polymer linear charge density.[15]

Figure 13 shows that the %BSA entrapped in the coacervate decreases with increasing ionic strength. The increased protein yield at low I is not surprising, in that a decrease in the ionic shielding should lead to stronger electrostatic interactions within the PPC. These enhanced interactions are reflected in the %water content of the coacervate, also shown in Figure 13. As the ionic strength is decreased, water is squeezed out and the PPC becomes more dense.

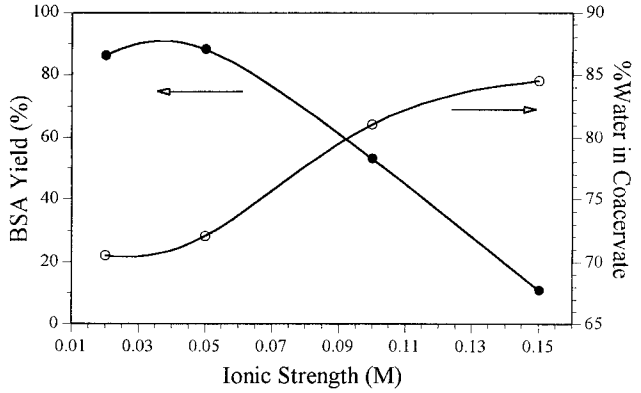


**Figure 13:** %BSA (●) and %$H_2O$ (O) in BSA-PDMDAAC coacervate prepared at pH 9, r = 5.

*Polyelectrolyte Chain Parameters*

Two key structural features of the polyelectrolyte chain are its charge density (charge per unit contour length) and its stiffness (parameterized by the persistence length).[32] Figure 14 shows $(Z_{pr})_c$ *vs.* $I^{½}$ phase boundaries[10] for BSA with PDMDAAC, PMAPTAC, PAMPS and the AMPS-acrylamide copolymer ($PAMPS_{80}AAm$). The charge density ($\xi$) and bare persistence length ($l_o$), representative of the intrinsic chain stiffness, of the polyelectrolytes are listed in Table 2 (see Figure 1 for structures).

**Table 2: Polyelectrolyte Chain Parameters[10]**

| | Charge Density, $\xi$ ($Å^{-1}$) | Base Persistence Length, $l_o$ (Å) |
|---|---|---|
| PMAPTAC | 2.8 | 24 |
| PAMPS | 2.8 | 24 |
| $PAMPS_{80}AAm$ | 2.3 | 24 |
| PDMDAAC | 1.2 | 27 |

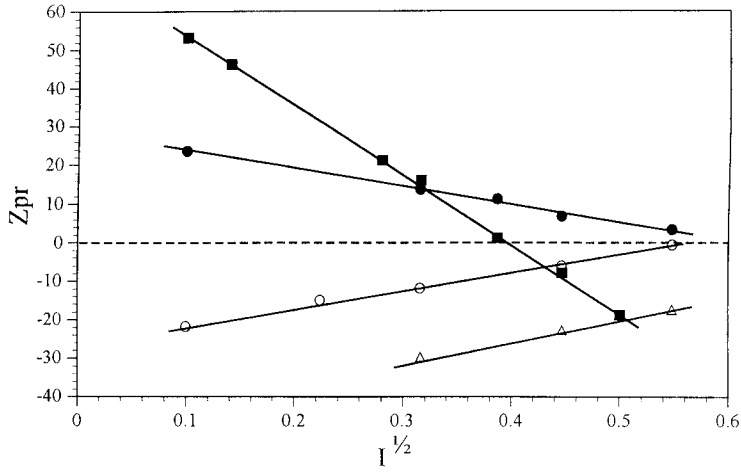


**Figure 14:** Ionic strength dependence of $(Z_{pr})_c$ for BSA with PMAPTAC (●), PAMPS (O), $PAMPS_{80}AAm$ (△), and PDMDAAC (■).

If protein charges were randomly distributed, one would expect symmetrical behavior for the binding of polyanions and polycations. This is exactly what we observe for the two high charge density polyelectrolytes, PMAPTAC and PAMPS. On the other hand, the lines for PMAPTAC and PDMDAAC cross. At low ionic strength, PDMDAAC binds more strongly, but vice versa at high I. Put differently, if the pH of a solution containing BSA, PMAPTAC and PDMDAAC were adjusted upwards at low I, complexation with PDMDAAC would occur prior to that with PMAPTAC, and contrariwise at high I. Figure 15 provides a schematic explanation. At low I, $pH_c < pI$, and the protein has a net positive charge. Nevertheless, bound configurations of PDMDAAC exist in which contacts between $NH_3^+$ and polymer cation sites are avoided because of the large spacing (≈7Å) between polymer charges. Unfavorable like-charge contacts would be less avoidable for PMAPTAC, which has more than twice the linear charge density of PDMDAAC. Consequently, PMAPTAC does not bind at large $Z_{pr}$ as well as PDMDAAC does. At high ionic strengths, $pH_\phi$ and the number of attractive $CO_2^-$ groups increases. The net result is an increase in the charge complementarity between PMAPTAC and a series of $CO_2^-$ groups on the protein surface, and preferential binding of BSA to the higher charge density PMAPTAC.

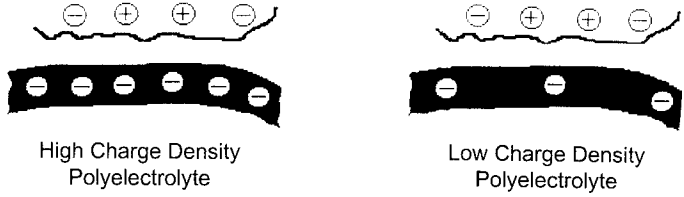


**Figure 15:** Schematic illustrating influence of charge complementarity on protein-polyelectrolyte interactions. Polyelectrolyte is shaded.

Comparison of PAMPS and $PAMPS_{80}AAm$ in Figure 13 indicates that intrinsic chain flexibility also plays a role in the binding of proteins to polyelectrolytes. The stronger binding by the lower charge density $PAMPS_{80}AAm$ can be explained on the basis of charge complementarity. However, the nearly parallel behavior of the two PAMPS polyelectrolytes in Figure 14, implies that the linear charge density has only a negligible influence on the ionic strength dependence of $(Z_{pr})_c$. This observation can be interpreted using Muthukumar's model for the adsorption of polyelectrolytes to charged surfaces.[28,29] The mathematical expression derived from the model is shown in Eq. 2, where $\sigma_c$ and $\Lambda$ are the critical surface charge density and radius of the protein charge patch, $\kappa$ is the Debye-Hückel parameter, and $l_o$ and $\xi$ are the polyelectrolyte bare persistence length and linear charge density respectively.

$$\sigma_c \sim \left( \frac{l_o^{0.6}}{\xi^{0.2}\Lambda} \right) \kappa^{1.2} \qquad (2)$$

Equation 2 predicts that the intrinsic stiffness of the polymer chain ($l_o$) will have a larger influence on $\sigma_c$ that the polyelectrolyte linear charge density. Therefore, the slopes of the phase boundaries ($\partial\sigma_c/\partial\kappa$) for PAMPS and $PAMPS_{80}AAm$, two polymers with similar bare persistence lengths, are nearly parallel, with the small difference in slopes arising from the difference in $\xi^{1.5}$. As discussed above, the vertical shift toward stronger binding for the copolymer is a result a charge complementarity or same sign charge repulsion, a factor not included in Muthukumar's model. For the polycations, Equation 2 correctly predicts that the phase boundary slope will be steeper for PDMDAAC than for PMAPTAC.

Even though they are treated as separate quantities in Equation 2, $\Lambda$, the protein patch radius, and $l_o$, the polymer bare persistence length, are fundamentally linked. The persistence length is representative of the number of polymer repeat units that are conformationally constrained. Because of these constraints, a set number of consecutive polymer sub-units are 'presented' to the protein as a single unit. For larger proteins then, $\Lambda$ should be proportional to $l_o$. $\Lambda$ will be limited however, by protein surface curvature and the hydrodynamic radius. Hence for smaller proteins, the importance of polyelectrolyte chain flexibility should be diminished. This prediction is consistent with PPC studies by Sato *et al.*, who observed no dependence of $pH_c$ on $\xi$ for the binding of lysozyme with $PAMPS_{80}AAm$.[33] In a like sense, highly flexible polymers lead to decreased values of $\Lambda$, and a potential loss in protein selectivity. These concepts are illustrated in Figure 16.

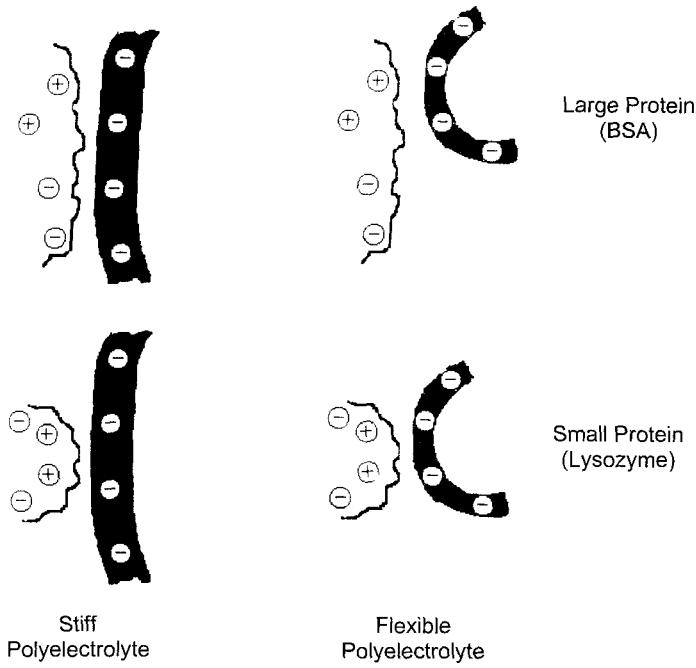


**Figure 16:** Schematics illustrating influence of polymer chain flexibility on PPC interactions. Polyelectrolyte is shaded.

## Conclusions

Protein-polyelectrolyte binding is initiated by electrostatic interactions between a small patch on the protein surface and a short segment of the polyelectrolyte chain. Protein binding is typically initiated on the wrong side of pI, indicating that the charge density of the protein patch is different from the global charge density. The electrostatic interactions in protein-polyelectrolyte systems are enhanced by a reduction in the salt content and changes in the solution pH, (e.g. an increase in pH for protein-polycation systems and decrease in pH for protein-polyanion systems), and while the composition of the complex is controlled by mass action, it also reflects these electrostatic interactions. In other words, the binding constant for protein-polyelectrolyte binding is modulated by an electrostatic parameter, with a change in either the pH or the ionic strength leading to a subsequent change in the number of proteins bound per polymer chain. This observation was recently verified by Hallberg *et al.*, using binding isotherms calculated from capillary electrophoresis.[34]

The size of the binding patch on the protein surface is determined by polyelectrolyte chain flexibility, i.e. the radius of the charge patch is proportional to the polyelectrolyte persistence length. As the patch radius increases, so does the influence of charge complementarity, in that the inclusion of non-complementary charges (same sign as the polyelectrolyte) within the protein charge patch can lead to repulsion of high charge density polymers and preferential binding to lower charge density polyelectrolytes. The net result is that protein selectivity, mass composition, and phase behavior in PPCs can all be controlled via the polyelectrolyte's statistical chain parameters. However, the radius of the charge patch is limited by the size of the protein. Hence, the influence of polymer chain flexibility on PPC composition may be significantly decreased for smaller proteins. In the same sense, highly flexible polymers can bind to smaller protein patches, leading to a potential loss in protein selectivity via the decreased influence of charge complementarity.

Bulk phase separation is a consequence of a decrease in solubility of the primary protein-polyelectrolyte complex (PPC). This insolubility mainly arises from charge neutralization within the primary complex. Therefore, phase separation is limited to solution conditions wherein the global protein charge is opposite in sign to that of the polyelectrolyte.

## Acknowledgments

This research was supported by National Science Foundation Grant DMR-9619772.

## References


1) Shaner, S.L.; Melancon, P.; Lee, K.S.; Burgess, R.R.; Record, M.T. Jr. *Cold Spring Harbor Symp. Quant. Biol.* **1983**, *47*, 463.
2) Colby, R.H. Poster presented at Gordon Conferance on "Colloidal, Macromolecular, and Polyelectrolyte Solutions, Ventura Ca., Feb 1998.
3) Xia, J.; Dubin, P.L. In *Macromolecular Complexes in Chemistry and Biology*; Dubin, P.L., Bock, J., Davis, R.M., Schulz, D., Thies, C., Eds,; Springer-Verlag: Berlin, 1994; Chapter 15.
4) Dubin, P.L.; Gao, J.; Mattison, K.W. *Sep. Purif. Methods* **1994**, *23*, 1.
5) Kokufuta, E. *Prog. Polym. Sci.* **1992**, *16*, 1.
6) Griffith, A.; Glidle, A.; Beamson, G.; Cooper, J.M. *J. Phys. Chem. B* **1997**, *101*, 2092.
7) Torchilin, V. In *Blood Substitutes: Industrial Opportunities and Medical Challenges*; Winslow, R.M., Vandegriff, K.D., Intaglietta, M., Eds,; Birkhaeuser: Boston, 1996; pg. 351.
8) Lim, F. In *Biomedical Applications of Microencapsulation*. CRC Press, Boca Raton, 1984.
9) Chang, T.M.S. *Biotechnol. Annu. Rev.* **1995**, *1*, 267.
10) Mattison, K.W.; Dubin, P.L.; Brittain, I.J. *J. Phys. Chem. B* **1998**, *102*, 3830.
11) Li, Y.; Mattison, K.; Dubin, P.L.; Havel, H.; Edwards, S. *Biopolymers* **1996**, *38*, 527.
12) Wen, Y.-P.; Dubin, P.L. *Macromolecules* **1997**, *30*, 7856.
13) Mattison, K.W.; Brittain, I.; Dubin, P.L. *Biotechnol. Prog.* **1995**, *11*, 632.
14) Strege, M.A.; Dubin, P.L.; West, J.S.; Daniel Flinta, C.D. In *Protein Purification: From Molecular Mechanisms to Large-Scale Processes*; Ladisch, M.; Wilson, R.C.; Painton, C.C.; Builder, S., Eds.; American Chemical Society: Washington DC, 1990; Chapter 5.
15) Okasaki, T.; Kaibara, K.; Maeda, H. In prep.
16) Bungenberg de Jong, M.G. In *Colloid Science (II), Reversible Systems*, Kruyt, G.R. Eds.; Elsevier, New York, 1949; pg. 335.
17) Burgess, D. In *Macromolecular Complexes in Chemistry and Biology*; Dubin, P.L., Bock, J., Davis, R.M., Schulz, D., Thies, C., Eds,; Springer-Verlag: Berlin, 1994; Chapter 17.
18) Burgess, D. *J. Colloid Interface Sci.* **1990**, *140* (1), 227.
19) Ahmed, L.; Xia, J.; Dubin, P.L.; Kokufuta, E. *J. Macro. Sci.-Pure Appl. Chem.* **1994**, *A31* (1), 17.
20) Tsuboi, A.; Tsuyoshi, I.; Hirata, M.; Xia, J.; Dubin, P.L.; Kokufuta, E. *Langmuir* **1996**, *12*, 6295.
21) Wang, Y.; Gao, J.Y.; Dubin, P.L. *Biotechnol. Prog.* **1996**, *12*, 356.
22) Xia, J.; Dubin, P.L.; Kim, Y.; Muhoberac, B.; Klimkowski, V.J. *J. Phys. Chem.* **1993**, *97*, 4528.
23) Zaitsev, V.S.; Izumrudov, V.A.; Zezin, A.B. *Polymer Science USSR* **1992**, *34* (1), 54.
24) Bowman, W.A.; Rubinstein, M.; Tan, J.S. *Macromolecules* **1997**, *30*, 3262.
25) Gao, J.; Dubin, P.L.; Muhoberac, B.B. *J. Phys. Chem. B*, submitted.

[26] Kabanov, V.A.; Evdakov, V.P.; Mustafaev, M.I.; Antipina, A.D. *Malokul. Biol.* **1977**, *11*, 582.
[27] Xia, J.; Dubin, P.L. *J. Chromatogr. A* **1994**, *667*, 311.
[28] Muthukumar, M. *J. Chem. Phys.* **1987**, *86*, 7230.
[29] Muthukumar, M. *J. Chem. Phys.* **1995**, *103*, 4723.
[30] Zhang, H.; Ray, J.; Manning, G.; Moorefield, C.; Newkome, G.; Dubin, P.L. *J. Phys. Chem.*, submitted.
[31] Evers, O.A.; Fleer, G.J.; Scheutjens, J.M.H.M.; Lyklema, J. *J. Colloid Interface Sci.* **1986**, *111*, 446.
[32] Yamakawa, H. *Modern Theory of Polymer Solutions*; Harper & Row: New York, **1971**.
[33] Sato,Takeshi; Mattison, Kevin W.; Dubin, Paul L.; Kamachi, Mikiharu; Morishima, Yotaro *Langmuir* **1998**, *14* (19), 5430.
[34] Hallberg, R.; Dubin, P.L. *J. Phys. Chem. B* **1998**, *102* (43), 8629.